Inorganic Chemistry

ARTICLE

pubs.acs.org/IC

Planar Tetranuclear Dy(III) Single-Molecule Magnet and Its Sm(III), Gd(III), and Tb(III) Analogues Encapsulated by Salen-Type and β-Diketonate Ligands

Peng-Fei Yan,[†] Po-Heng Lin,[‡] Fatemah Habib,[‡] Tomoko Aharen,[‡] Muralee Murugesu,*[,‡] Zhao-Peng Deng,[†] Guang-Ming Li,[†] and Wen-Bin Sun*[,†,§]

[†]Key Laboratory of Functional Inorganic Material Chemistry, Heilongjiang University, Ministry of Education, No. 74, Xuefu Road, Nangang District, Harbin 150080, P.R. China

[‡]Department of Chemistry, University of Ottawa, 10 Marie Curie, Ottawa, Ontario, K1N6N5, Canada

[§]Key Laboratory of Chemical Engineering Process & Technology for High-efficiency Conversion, College of Heilongjiang Province, No. 74, Xuefu Road, Nangang District, Harbin 150080, P.R. China

Supporting Information

ABSTRACT: The syntheses, structures, and magnetic properties are reported for four new lanthanide clusters $[Sm_4(\mu_3\text{-}OH)_2L_2(acac)_6]\cdot 4H_2O$ (**1**), $[Gd_4(\mu_3\text{-}OH)_2L_2(acac)_6]\cdot 4CH_3CN$ (**2**), and $[Ln_4(\mu_3\text{-}OH)_2L_2(acac)_6]\cdot 2H_2L\cdot 2CH_3CN$ (**3**, Ln = Tb; **4**, Ln = Dy) supported by salen-type (H_2L = *N*,*N*′-bis(salicylidene)-1,2-cyclohexanediamine) and β-diketonate (acac = acetylacetonate) ligands. The four clusters were confirmed to be essentially isomorphous by infrared spectroscopy and single-crystal X-ray diffraction. Their crystal structures reveal that the salen-type ligand provides a suitable tetradentate coordination pocket (N_2O_2) to encapsulate lanthanide(III) ions. Moreover, the planar Ln_4 core is bridged by two μ_3-hydroxide, four phenoxide, and two ketonate oxygen atoms. Magnetic properties of all four compounds have been investigated using dc and ac susceptibility measurements. For **4**, the static and dynamic data indicate that the Dy_4 complex exhibits slow relaxation of the magnetization below 5 K associated with single-molecule magnet behavior.

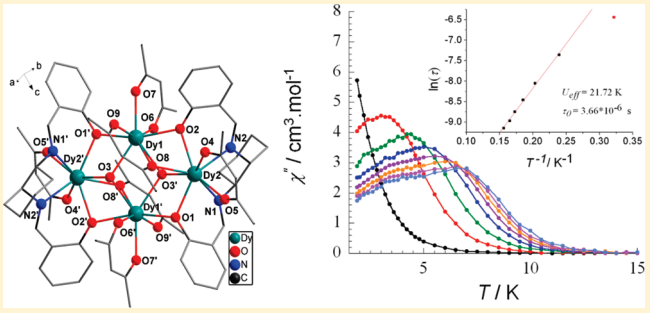

INTRODUCTION

Single-molecule magnets (SMMs) exhibiting slow relaxation of the magnetization have recently attracted much attention due to their potential application in high-density information storage, quantum computing, and molecular spintronics.[1−4] SMMs are discrete magnetic clusters which generally possess a large spin ground state (*S*) in combination with a large uniaxial magnetic anisotropy (*D*) leading to an anisotropic energy barrier (*U*) for reversal of the magnetization. Most of the reported SMMs are based on polynuclear 3*d* metal aggregates, especially large manganese complexes[5,6] where the uniaxial anisotropy results from Jahn−Teller elongated Mn(III) ions. Thus, after the discovery of many first-row transition-metal-based SMMs, the focus in this research field was redirected toward mixed 3*d*−4*f* clusters as well as pure 4f-based systems as new SMMs.[7] This is due to the large spin−orbit coupling observed in lanthanide ions which increases the *D* value for the complex resulting in higher energy barriers compared to SMMs with 3*d* metals.[7] Among them, lanthanide ions such as Dy(III) and Tb(III) are widely studied due to their large intrinsic magnetic anisotropy and reduced quantum tunneling of the magnetization (QTM).[8,9] Although the magnetic coupling in these systems is likely weak, 4*f* SMMs will possess larger energy barriers provided the principal magnetic axes are ideally oriented.[10a] In such SMMs the energy barrier mainly rises from the single-ion anisotropy.[11] Considerable effort has been dedicated to the investigation of 4*f*-based clusters, most of which contain tetranuclear Dy(III) ions with cubane[12−16] and planar metal cores.[7a,10] In comparison with 3*d*-based SMMs, far fewer 4*f* SMMs have been reported owing to the difficulty in promoting magnetic interactions between the bridging ligand orbitals and the 4*f* orbitals of the lanthanide ions.[8a,9a]

Organic ligands used in the synthesis of discrete SMMs play multiple roles: (i) ligating/encapsulating the metal centers, (ii) preventing intermolecular interactions by isolating molecular entities, (iii) dictating the structural arrangement, and (iv) promoting intramolecular magnetic interactions via superexchange pathways. The latter feature is critical for 4*f* SMMs as the buried magnetic 4*f* orbitals do not overlap well with the bridging ligand orbitals.[10] Bulky, multidentate ligands such as polyalcohols, carboxylic acid derivatives, oximate derivatives, and Schiff-base ligands were successfully employed in isolation of

Received: March 19, 2011

   dx.doi.org/10.1021/ic200566y | *Inorg. Chem.* XXXX, XXX, 000–000

high-energy barrier SMMs.[17] With this in mind, our synthetic strategy involved both salen-type and β-diketonate ligands (Scheme 1) in order to isolate polynuclear lanthanide cluster complexes.

Although the tetradentate salen-type ligands have been widely used to synthesize $3d-4f$ molecular magnets, previous studies indicated that the lanthanide ions did not favor binding in the inner N_2O_2 coordination pocket.[18] As hard Lewis acids with high oxophilicity, lanthanide ions do not favor coordination with soft Lewis-base N atoms and therefore an ancillary β-diketonate ligand with steric hindrance was selected. Along with promoting spatial isolation of the Ln_4 clusters it also pushes the lanthanide ions into the N_2O_2 coordination pocket of H_2L ligand. Additionally, this satisfies the required high coordination numbers of Ln(III) ions. A series of four planar tetranuclear Sm(III) (**1**), Gd(III) (**2**), Tb(III) (**3**), and Dy(III) (**4**) clusters were successfully synthesized using β-diketonate and salen-type ligands. The obtained tetranuclear complexes are isostructural; however, due to the unique intrinsic properties of the employed lanthanide ions, their magnetic behaviors are dissimilar. Herein, we report the preparation, structural description, and magnetic properties of a series of Ln_4 clusters with SMM behavior observed in the Dy_4 analogue.

EXPERIMENTAL SECTION

General Information. All chemicals and solvents were obtained from commercial sources and used as received without further purification. Elemental (C, H, and N) analyses were performed on a Perkin-Elmer 2400 analyzer. Fourier transform IR spectra were measured on a Perkin-Elmer Spectrum One spectrometer with samples prepared as KBr pellets. The salen-type ligand *N,N′*-bis(salicylidene)-1,2-cyclohexanediamine (H_2L) was obtained by condensation of 1,2-cyclohexanediamine and salicylaldehyde in a 1:2 molar ratio in absolute methanol, according to previously reported synthetic methods.[19] The lanthanide precursors, $Ln(acac)_3 \cdot H_2O$, where Ln = Sm(III), Gd(III), Tb(III), and Dy(III), were prepared according to a literature procedure previously described.[20]

Scheme 1. Representation of the ligands H_2L (left) and acac (right)

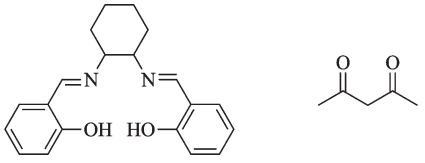

Synthesis of $[Dy_4(\mu_3\text{-}OH)_2L_2(acac)_6]\cdot 2H_2L\cdot 2CH_3CN$ (4). The same procedure was employed in preparing all complexes; hence, only compound **4** will be described in detail. To 10 mL of an acetonitrile solution of H_2L (0.338 g, 1.0 mmol) was slowly added 10 mL of a methanol solution of $Dy(acac)_3 \cdot H_2O$ (0.485 g, 1.0 mmol) under stirring. The solution was refluxed for 3 h, and the filtrate was allowed to crystallize at room temperature by slow evaporation. Yellow crystals, suitable for single-crystal X-ray diffraction analysis, were obtained after 2 weeks.

Elemental Analyses, Infrared, and Yields for Complexes 1−4. Anal. Calcd for $C_{70}H_{92}N_4O_{22}Sm_4$ (**1**): C, 43.27; H, 4.77; N, 2.88. Found: C, 43.19; H, 4.45; N, 2.57. Anal. Calcd for $C_{78}H_{96}Gd_4N_8O_{18}$ (**2**): C, 45.42; H, 4.69; N, 5.43. Found: C, 45.30; H, 4.55; N, 5.39. Anal. Calcd for $C_{114}H_{138}N_{10}O_{22}Tb_4$ (**3**): C, 51.94; H, 5.28; N, 5.31. Found: C, 51.79; H, 5.05; N, 5.01. Anal. Calcd for $C_{114}H_{138}Dy_4N_{10}O_{22}$ (**4**): C, 51.66; H, 5.25; N, 5.28. Found: C, 51.64; H, 5.82; N, 5.27. IR (KBr, cm^{-1}) for **1**: 3400 (br), 1625 (br), 1604 (s), 1515 (s), 1391 (s), 1259 (m), 1016 (w), 918 (w), 757 (m), 652 (w). IR (KBr, cm^{-1}) for **2**: 3429 (br), 1624 (s), 1603 (s), 1517 (s), 1386 (s), 1288 (m), 1017 (w), 921 (w), 754 (m), 620 (w). IR (KBr, cm^{-1}) for **3**: 3430 (br), 2246 (w), 1626 (s), 1601 (s), 1516 (s), 1391 (s), 1291 (m), 1021 (w), 923 (w), 757 (m), 623 (w). IR (KBr, cm^{-1}) for **4**: 3425 (br), 2239 (w), 1629 (s), 1603 (s), 1519 (s), 1386 (s), 1289 (m), 1019 (w), 923 (w), 747 (m), 627 (w). Yields = 37−45%.

X-ray Crystallographic Analysis and Data Collection. Single-crystal X-ray data of the four clusters were collected at 293 K on a

Table 1. Crystallographic Data and Structure Refinement for Complexes 1−4

	1	2	3	4
empirical formula	$C_{70}H_{92}N_4O_{22}Sm_4$	$C_{78}H_{96}N_8O_{18}Gd_4$	$C_{114}H_{138}N_{10}O_{22}Tb_4$	$C_{114}H_{138}N_{10}O_{22}\ Dy_4$
fw ($g\cdot mol^{-1}$)	1942.81	2062.63	2636.02	2650.34
cryst syst	monoclinic	triclinic	triclinic	triclinic
space group	$C2/c$	$P\bar{1}$	$P\bar{1}$	$P\bar{1}$
temp. (K)	293(2)	293(2)	293(2)	293(2)
a (Å)	27.1629(17)	11.8151(8)	13.5830(18)	13.5657(14)
b (Å)	15.3001(11)	14.4643(10)	14.1528(19)	14.1614(15)
c (Å)	20.3369(11)	14.7798(10)	16.344(2)	16.3381(17)
α (deg)	90	106.3820(10)	80.304(2)	80.3610(10)
β (deg)	99.4480(10)	110.8000(10)	71.039(2)	70.8770(10)
γ (deg)	90	103.2960(10)	74.676(2)	74.7040(10)
V ($Å^3$)	8337.3(9)	2106.3(2)	2854.0(7)	2849.1(5)
ρ_{calcd} ($Mg\cdot m^{-3}$)	1.540	1.626	1.534	1.540
μ (mm^{-1})	2.843	3.176	2.520	2.664
$F(000)$	3816	1020	1328	1324
collected reflns	25 661	19 131	24 078	25 040
independent reflns	9232	9906	13 549	13 555
R_{int}	0.0616	0.0391	0.0390	0.0224
$R1$ [$I > 2\sigma(I)$]	0.0645	0.0426	0.0465	0.0319
$wR2$ (all data)	0.2441	0.0956	0.1268	0.0845
goodness-of-fit on F^2	1.008	0.989	0.997	1.051

dx.doi.org/10.1021/ic200566y |*Inorg. Chem.* XXXX, XXX, 000–000

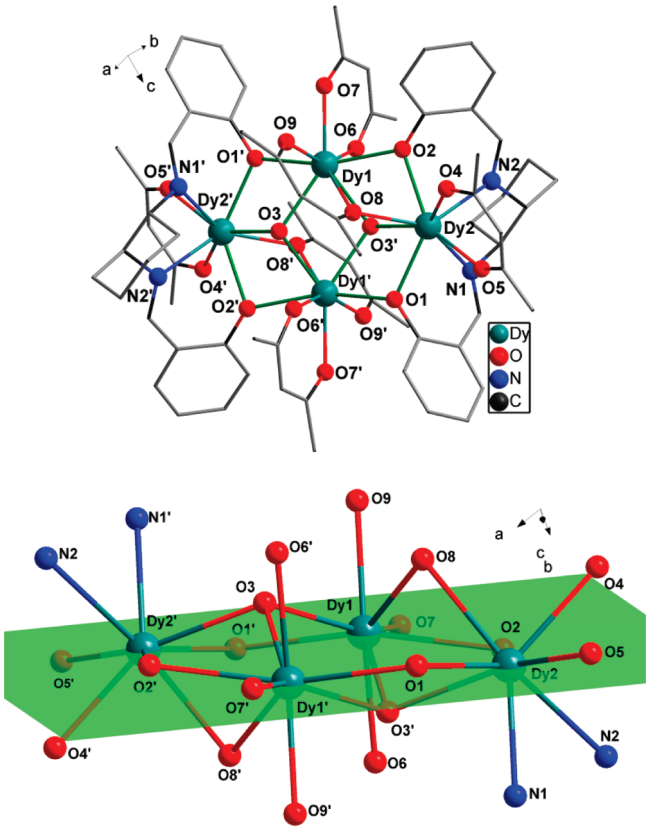

Figure 1. Molecular structure of **4** (top), and side view of the planar Dy_4 core (bottom). All hydrogen atoms and dissociative molecules have been omitted for clarity. Color code: green (Dy), blue (N), red (O), gray (C).

Bruker SMART CCD diffractometer equipped with graphite-monochromatized Mo Kα radiation (λ = 0.71073 Å). Multiscan absorption corrections were applied using the SADABS program.[21] The structure was solved by direct and Patterson methods and refined by full-matrix least-squares methods on F^2, which were performed using the SHELXTL-97 software package.[22] The location of the lanthanide atoms was easily determined, and O, N, C, and H atoms were subsequently determined from the difference Fourier maps. The non-hydrogen atoms were refined anisotropically. The H atoms were introduced in calculated positions and refined with fixed geometry with respect to their carrier atoms. All of the crystal data and structure refinement details for these four compounds are summarized in Table 1. Selected bond lengths and angles for **1**−**4** are listed in Table S1, Supporting Information. Crystallographic data for all structures can be obtained from the Cambridge Crystallographic Data Centre as supplementary publication nos. CCDC 801788 (**1**), 801786 (**2**), 806975 (**3**), and 801787 (**4**).

Magnetic Measurements. The magnetic susceptibility measurements were obtained using a Quantum Design SQUID magnetometer MPMS-XL 7 operating between 1.8 and 300 K for dc-applied fields ranging from −7 to 7 T. dc analyses were performed on polycrystalline samples of 12.8, 10.9, 13.2, and 12.2 mg for **1**, **2**, **3**, and **4**, respectively, wrapped in a polyethylene membrane. ac susceptibility measurements were carried out under an oscillating ac field of 3 Oe and ac frequencies ranging from 1 to 1500 Hz. Magnetization data were collected at 100 K to check for ferromagnetic impurities that were absent in all samples. A diamagnetic correction was applied for the sample holder.

RESULTS AND DISCUSSION

Synthesis. All compounds were synthesized by refluxing the ligand *N,N′*-bis(salicylidene)-1,2-cyclohexanediamine (H_2L) and $Ln(acac)_3 \cdot H_2O$ (1:1 molar ratio) in a mixture of methanol/acetonitrile (10:10 mL). It is noteworthy that *N,N′*-bis-(salicylidene)-1,2-cyclohexanediamine acts not only as a ligand in this reaction but also as the base, thus promoting formation of hydoxide ligands from water molecules introduced by the starting materials. A similar bifunctional ligand was reported in the literature.[7a] Moreover, changes to the molar ratio between ligand and $Ln(acac)_3 \cdot H_2O$ as well as using a single solvent system such as MeOH or MeCN result in noncrystalline materials.

Structural Analysis. Single-crystal X-ray diffraction, IR analysis (Figure S1, Supporting Information), and charge-balance considerations indicate that complexes **1**−**4** are essentially isomorphous, with the same tetranuclear $[Ln_4(\mu_3{-}OH)_2L_2(acac)_6]$ core. They differ, however, in their dissociative neutral molecules as shown in their formulas. A partially labeled complex **4** with a crystallographically centrosymmetric Dy_4 core is depicted in Figure 1.

As shown in Figure 1, all 8-coordinate Dy(III) ions are coplanar and linked together by a combination of μ_3-hydroxo (O3, O3′), ketonate (O8, O8′), and phenoxo (O1, O2, O1′, O2′) oxygen atoms. The Dy2 and Dy2′ ions are located in the inner coordination N_2O_2 pocket (Figure S2, Supporting Information) of two salen-type ligands with Dy2−N1, Dy2−N2, Dy2−O1, and Dy2−O2 distances equal to 2.507(3), 2.518(4), 2.361(3), and 2.381(3) Å, respectively. Two triply bridging hydroxide (O3, O3′) atoms lie approximately 0.90 Å above and below the Dy_4 plane (Figure 1 bottom). Such planar Dy_4 complexes are relatively rare in the literature with only three other examples currently reported.[7a,10] The μ_3-OH groups form near symmetrical bridges to the metal centers, with Dy2−O3, Dy1′−O3, and Dy1−O3 distances of 2.342(2), 2.340(3), and 2.378(2) Å, respectively, as well as Dy1′−O3−Dy2′, Dy1′−O3−Dy1, and Dy2′−O3−Dy1 angles of 102.09(9)°, 106.63(9)°, and 109.69(10)°, respectively (Table S1, Supporting Information). There are six anionic $acac^-$ ligands above and below the planar core chelating to four Dy(III) ions. In the centrosymmetric complex the 8-coordinate Dy1 and Dy2 ions display a distorted square-antiprismatic geometry (Figure 2, top and middle). The Dy1 ions are coordinated exclusively to eight oxygen atoms, while six oxygen atoms and two soft imine nitrogen atoms form the coordination sphere around Dy2. The two square bases of the square antiprism for Dy1 consist of O2, O7, O9, O8 and O1′, O3, O3′, O6, whereas for Dy2, the two square bases are defined by the atoms O1, O5, O4, O8 and N1, N2, O2, O3′ (Figure 2, bottom; Figures S3 and S4, Supporting Information).

In a square antiprism, the parameter α could be used to describe the elongation or flatness (Figure 2, bottom).[12,23] α is the angle between the S_8 axis of the square antiprism and the central atom ligand bond which is also defined as $\alpha = \gamma/2$, where γ is the angle between opposite ligands within one hemisphere. A soft-sphere model results in the ideal α value of 57.16° if a repulsion energy law of $1/r^6$ is assumed. In **4**, the Dy1 ions are surrounded exclusivelyby O atoms with γ angles of 128.45(9)° (O7−Dy1−O8), 100.92(10)° (O9−Dy1−O2), 113.26(9)° (O3′−Dy1−O1′), and 117.74(9)° (O6−Dy1−O3) (Table S1, Supporting Information). The hemisphere including the atoms O2, O7, O8, and O9 is strongly distorted since the angles $\alpha_{(O7,O8)}$ = 64.23(9)° and $\alpha_{(O9,O2)}$ = 50.46(10)° are strongly

dx.doi.org/10.1021/ic200566y |*Inorg. Chem.* XXXX, XXX, 000–000

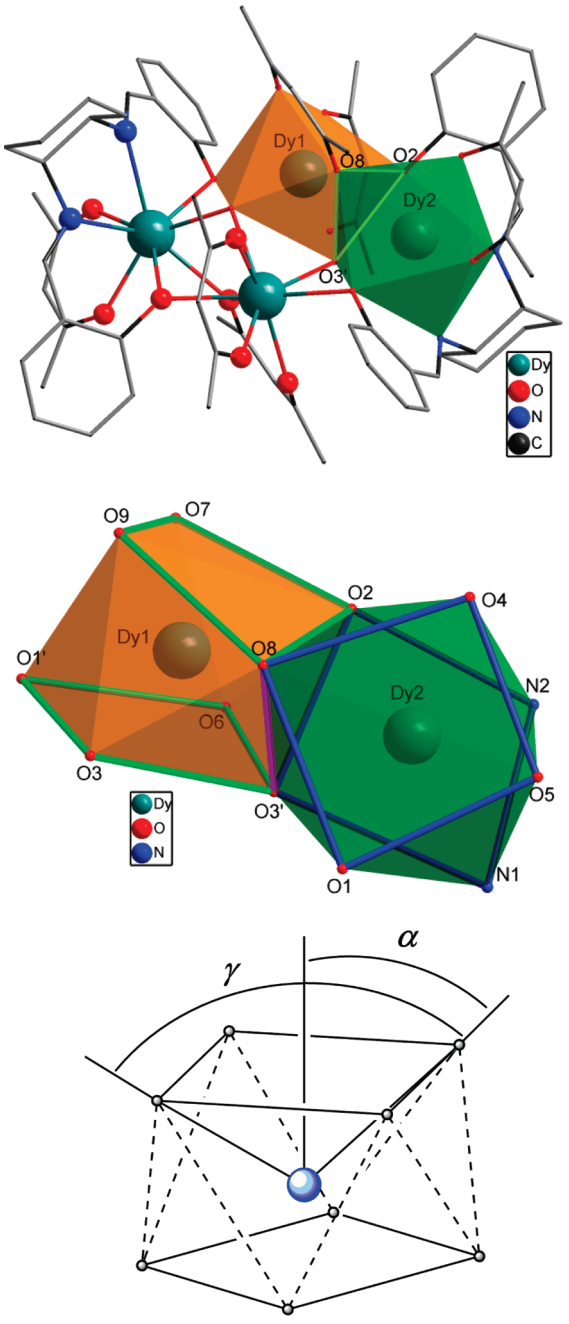

Figure 2. Molecular structure of **4**, illustrating the Dy_4 planar core (top), coordination polyhedra for the adjacent Dy(III) ions (middle), and definition of the angle α in a regular square antiprism (bottom), where γ is the angle between opposite ligands within on hemisphere: $\alpha = \gamma/2$.

deviated from the theoretical values by 7.1° and 6.7° for a square antiprism. This distortion is most likely due to the small bite angle of μ_3-OH ligands (O3′—Dy1—O3 = 73.37(9)°). The second hemisphere with $\alpha_{(O3',O1')}$ = 56.63(9)° and $\alpha_{(O6,O3)}$ = 58.87(9)° are close to the ideal values for a square antiprism. However, for the Dy2 ions the γ angles are 125.14(10)° (O4—Dy2—O1), 120.62(10)° (O5—Dy2—O8), 123.09(11)° (O2—Dy2—N1), and 103.23(10)° (O3′—Dy2—N2), while the α angles are 62.57(10)°, 60.32(10)°, 61.55(11)°, and 51.62(10)°, indicating strong distortion from ideal values. This is most likely due to the constraints imposed on Dy2 ions in the inner N_2O_2 pockets. The two square antiprisms share three oxygen atoms, O2, O3′, and O8, which form a near isosceles triangular face (Figure 2 middle) with distances of 2.68, 2.69, and 2.75 Å for O8···O2, O8···O3′, and O2···O3′, respectively.

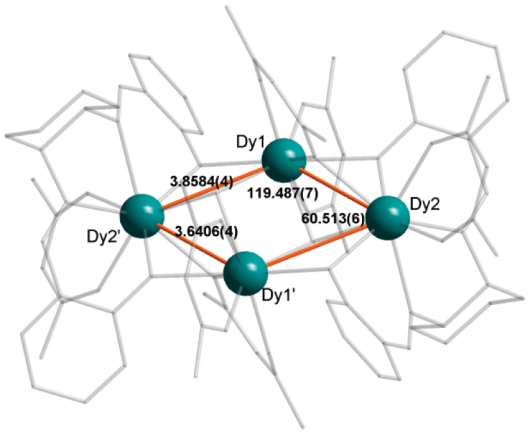

Figure 3. Parallelogram view consisting of four Dy(III) ions with edge distances (Å) and angles (deg) indicated.

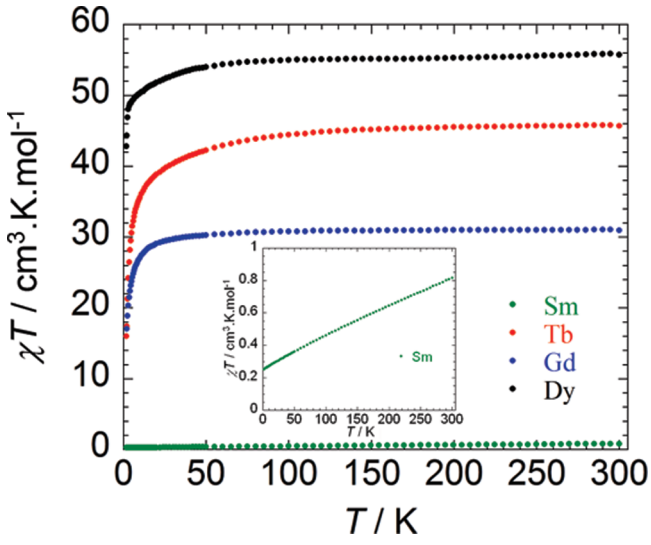

Figure 4. Temperature dependence of the χT product for all four complexes with an applied field of 1000 Oe. (Inset) Zoomed-in data of the temperature dependence of the χT product for the Sm_4 complex.

Finally, the four Dy(III) ions are located at the corners of a parallelogram with distances and angles between the metal centers described in Figure 3. All of the Dy—O distances in **4** are in the range of 2.284(3)—2.543(3) Å, and the O—Dy—O angles are in the range of 65.86(9)—158.10(9)°. The shortest intramolecular Dy···Dy distance of 3.6406(4) Å is on the edge of the parallelogram (Figure 3) between Dy1 and Dy2 as well as Dy1′ and Dy2′.

The four lanthanide complexes based on both lighter and heavier lanthanides (Sm(III) (**1**), Gd(III) (**2**), Tb(III) (**3**), Dy(III) (**4**)) essentially exhibit isostructural tetranuclear planar cores. The difference is due to dissociative neutral ligands present in **3** and **4** which are replaced by solvent molecules (MeCN and H_2O) in **1** and **2**.

dx.doi.org/10.1021/ic200566y |*Inorg. Chem.* XXXX, XXX, 000–000

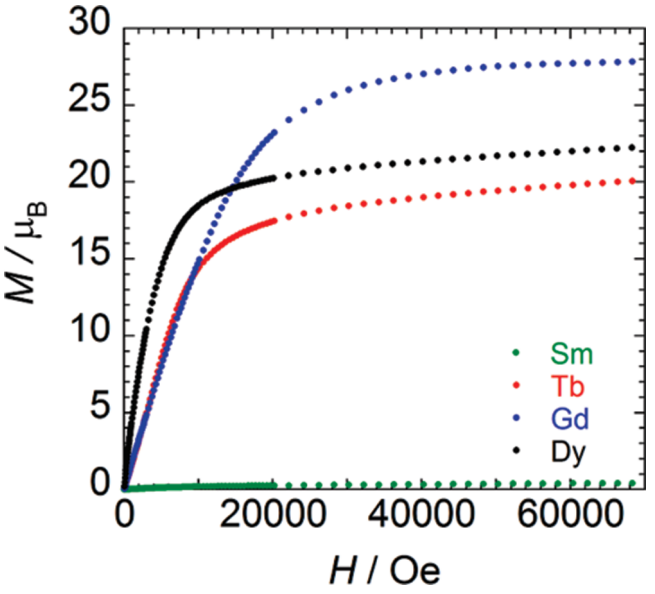

Figure 5. Magnetization as a function of field plot for all four complexes at 1.8 K.

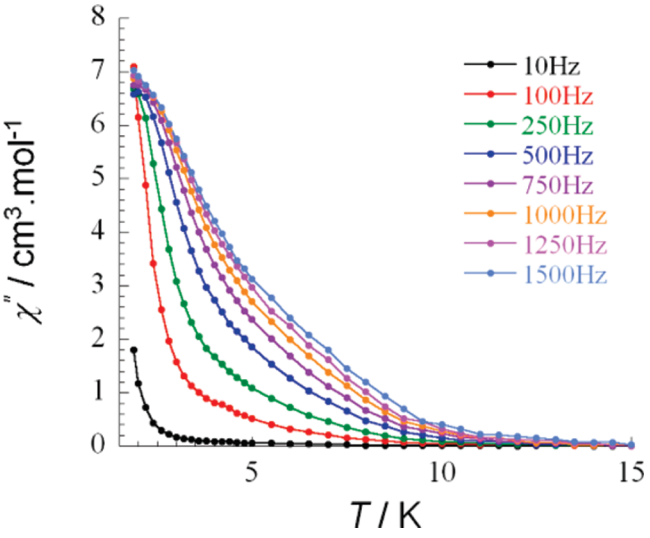

Figure 6. Frequency dependence of the out-of-phase ac susceptibility (χ'') between 10 and 1500 Hz at H_{dc} = 0 Oe for **4**.

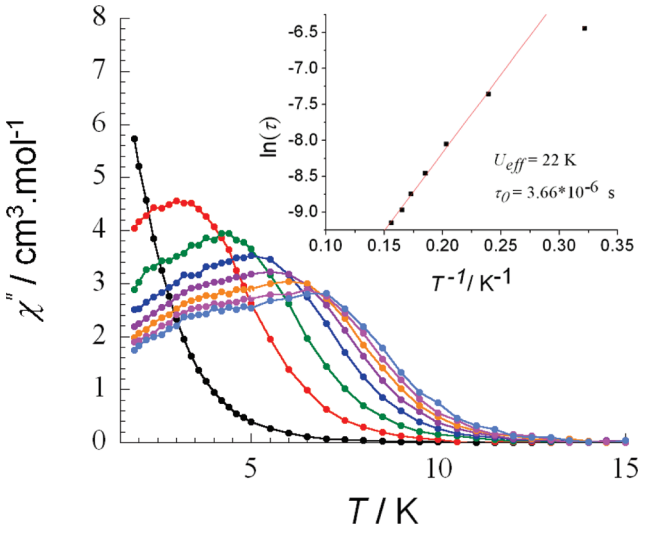

Figure 7. Frequency dependence of the out-of-phase ac susceptibility (χ'') between 10 and 1500 Hz at H_{dc} = 1400 Oe for **4**. (Inset) Relaxation time of the magnetization ln(τ) vs T^{-1} (Arrhenius plot using ac data) for **4**. The line corresponds to the fit.

Magnetic Properties. The dc magnetic measurements were performed on polycrystalline samples of **1**, **2**, **3**, and **4** between 1.8 and 300 K under an external field of 1000 Oe (Figure 4). The field dependence of the magnetization for all four complexes in the temperature range of 1.8−8 K were also obtained and are shown in Figures S5−S12, Supporting Information. The observed paramagnetic behaviors of all four complexes arise from the 4*f* Ln(III) ions. The experimentally obtained χT values are 0.82, 32.89, 45.68, and 55.71 $cm^3 \cdot K \cdot mol^{-1}$ for complexes **1**, **2**, **3**, and **4**, respectively. According to the free-ion approximation of each lanthanide ion, Sm(III) ($^6H_{5/2}$, $S = 5/2$, $L = 5$, $g = 2/7$, $\chi T = 0.09$ $cm^3 \cdot K \cdot mol^{-1}$), Gd(III) ($^8S_{7/2}$, $S = 7/2$; $L = 0$, $g = 2$, $\chi T = 7.88$ $cm^3 \cdot K \cdot mol^{-1}$), Tb(III) ($^7F_6$, $S = 3$, $L = 3$, $g = 3/2$, $\chi T = 11.82$ $cm^3 \cdot K \cdot mol^{-1}$), Dy(III) ($^6H_{15/2}$, $S = 5/2$, $L = 5$, $g = 4/3$, $\chi T = 14.17$ $cm^3 \cdot K \cdot mol^{-1}$), the theoretical value for four noninteracting lanthanide ions are calculated to be 0.36, 31.52, 47.28, and 56.68 $cm^3 \cdot K \cdot mol^{-1}$ for **1**, **2**, **3**, and **4**, respectively. The experimental χT value observed for **1** is slightly higher than the expected value due to low-lying excited states which can be easily populated at room temperature (Figure 4, inset). A plot of χT vs T is presented in Figure 4, where the x axis has been expanded to illustrate the experimental χT value. The observed values at room temperature for **2**, **3**, and **4** are close to the theoretical values. Upon decreasing the temperature the χT product remains fairly constant down to ∼50 K for **2** before dropping rapidly down to 17.03 $cm^3 \cdot K \cdot mol^{-1}$ at 1.8 K. Due to the isotropic nature of Gd(III) ions it is reasonable to assume the latter behavior is indicative of intramolecular antiferromagnetic interactions. Generally, for small spin tetranuclear complexes the magnitude of the interactions can be obtained by fitting the dc data using Kambe's vector coupling method. However, the presence of large spins (28 electrons), 4096 M_s states, and a coupling scheme involving a two J problem make derivation of the van Vleck equation horrendous. Therefore, in order to simplify this method the exchange coupling constants were assumed to be equal (one J problem). A reasonable fit was obtained (Figure S13, Supporting Information) with this approximation. The obtained J value of −0.02 cm^{-1} clearly suggests a weak antiferromagnetic exchange interaction via superexchange pathways. In the case of **3** and **4** the negative deviation starts to occur at slightly higher temperatures (∼75 K) before reaching 15.98 and 42.83 $cm^3 \cdot K \cdot mol^{-1}$, respectively, at 1.8 K. This is most likely due to a combination of antiferromagnetic interactions, thermal depopulation of Stark sublevels, and the presence of significant magnetic anisotropy.

Magnetization and reduced magnetization data for all complexes are given in Figure 5 and Figures S5−12, Supporting Information. The magnetization measurement for complex **2** (Figure 5) shows near saturation at $M = 27.84$ μ_B with an applied field of 7 T. This value is close to the expected theoretical value of 28.00 μ_B ($g = 2$). The magnetization measurements for complexes **1**, **3**, and **4** (Figure 5) show a relatively rapid increase below ∼1 T and slow linear increase without complete saturation up to 7 T. Their magnetization values (0.41, 20.13, and 22.28 μ_B)

dx.doi.org/10.1021/ic200566y |*Inorg. Chem.* XXXX, XXX, 000–000

are lower than their theoretically derived values (2.86, 36.00, and 40.00 μ_B for **1**, **3**, and **4**, respectively). As aforementioned, the complexes may have low-lying excited states or significant magnetic anisotropy resulting in large differences between experimental and theoretical values. Further confirmation was obtained with the M vs H/T plots (Figures S9−S12, Supporting Information); since all curves were not superimposed on a single master curve as expected for an isotropic system with a well-defined ground state we can conclude the presence of low-lying excited states or significant magnetic anisotropy.

Due to the presence of significant magnetic anisotropy and unpaired electrons in molecular lanthanide systems, complexes **3** and **4** may behave as SMMs. In order to verify their potential SMM behavior alternating current (ac) magnetic susceptibility studies were carried out on freshly filtered samples of **3** and **4**. Such measurements were generally carried out in the temperature range 1.8−10 K with a zero dc field and a 3.5 Oe ac field oscillating at frequencies between 10 and 1500 Hz. For complex **3** no out-of-phase signal (χ'') was observed even after a static dc field was applied. This behavior may be due to the quantum tunnelling of the magnetization (QTM) commonly seen in pure lanthanide polynuclear complexes.[7a,9a] For complex **4** a frequency-dependent signal was observed in the χ'' vs T plot below 10 K (Figure 6). This suggests slow relaxation of the magnetization, which is generally attributed to an SMM. However, relaxation barriers cannot be extracted from this data as no full peak was observed. In lanthanide systems, the tail of a peak generally indicates the presence of QTM, which reduces the expected energy barrier. It is possible to shortcut the QTM by applying a static dc field. Therefore, ac susceptibility measurements were obtained under a static dc field (Figure 7). The thermal dependence below 10 K of χ'' under an optimum field of 1400 Oe reveals one broad peak which is likely due to overlap of two distinct peaks with two relaxation modes. The Cole−Cole plot[24] in the temperature range of 2.5−6 K illustrates a switch from fairly symmetrical semicircles at high temperatures to semicircles with a slight shoulder at low temperatures (Figure S14, Supporting Information). If one relaxation process is present, the data could be fitted using a generalized Debye model with a mean α parameter value between 0 and 1.[25] In this case, however, no reasonable fit was obtained, which is indicative of the presence of two relaxation processes. The two relaxation modes can be attributed to two types of Dy(III) ions (Dy1, Dy2) in the centrosymmetric complex. We recently reported this type of behavior for another Dy_4 cluster.[10b] From this data we were able to extract the relaxation time for the higher temperature peak. The data was fitted yielding an effective spin-reversal barrier of U_{eff} = 22 K and a pre-exponential factor of $\tau_0 = 3.66 \times 10^{-6}$ s in the optimal field of 1400 Oe (Figure 7, inset). Such observation confirms the "field-induced" SMM nature of **4**. It is note worthy that although Tb(III) ($^7F_6$, $S = 3$, $L = 3$) and Dy(III) ($^6H_{15/2}$, $S = 5/2$, $L = 5$) ions are highly anisotropic with a large number of unpaired electrons only the Dy_4 complex exhibits slow relaxation of the magnetization. This is mainly due to the spin parity effect,[26] which indicates that QTM at zero field is suppressed for half integer spins. This further confirms the observed single-ion relaxation mechanism for **4** due to weak coupling between the 4*f* metal centers.

CONCLUSION

A planar tetranuclear Dy(III) SMM and its Sm(III), Gd(III), and Tb(III) analogues were prepared as well as characterized structurally and magnetically. The structural analyses demonstrated that the use of salen-type and β-diketonate ligands is ideal for isolation of planar tetranuclear lanthanide clusters in which the tetradentate N_2O_2 coordination pocket of salen-type ligands encapsulates the metal ions. This provides a synthetic strategy for isolation of planar-type tetranuclear lanthanide clusters incorporating diverse salen-type and β-diketonate analogues. This also presents an opportunity to tune the magnetic properties of these SMMs by modifying the encapsulating and bridging ligands. In order to confirm these assumptions, our current work focuses on accentuating the distortion of the core by using more rigid or soft salen-type and β-diketonate ligands with more pronounced steric hindrance.

ASSOCIATED CONTENT

Supporting Information. Crystallographic data in CIF format, IR spectra, additional figures, and magnetic data. This material is available free of charge via the Internet at http://pubs.acs.org.

AUTHOR INFORMATION

Corresponding Author

*E-mail: m.murugesu@uottawa.ca (M.M.), wenbinsun@yahoo.cn (W.B.S.).

ACKNOWLEDGMENT

This work was financially supported by the NNSF of China (21072049 and 50903028) and Educational Committee of Heilongjiang Province (10td03 and 11551336) and Heilongjiang University (QL201021 and Hdtd2010-08), NSERC, CFI.

REFERENCES

(1) Thomas, L.; Lionti, F.; Ballou, R.; Gatteschi, D.; Sessoli, R.; Barbara, B. *Nature* **1996**, *383*, 145.

(2) Leuenberger, M. N.; Loss, D. *Nature* **2001**, *410*, 789.

(3) Hill, S.; Edwards, R. S.; Aliaga-Alcalde, N.; Christou, G. *Science* **2003**, *302*, 1015.

(4) (a) Bogani, L.; Wernsdorfer, W. *Nat. Mater.* **2008**, *7*, 179. (b) Mannini, M.; Pineider, F.; Danieli, C.; Totti, F.; Sorace, L.; Sainctavit, Ph.; Arrio, M.-A.; Otero, E.; Joly, L.; Cezar, J. C.; Cornia, A.; Sessoli, R. *Nature* **2010**, 417. (c) Mannini, M.; Pineider, F.; Sainctavit, P.; Danieli, C.; Otero, E.; Sciancalepore, C.; Talarico, A. M.; Arrio, M.-A.; Cornia, A.; Gatteschi, D.; Sessoli, R. *Nat. Mater.* **2009**, *8*, 194.

(5) (a) Sessoli, R.; Gatteschi, D.; Caneschi, A.; Novak, M. A. *Nature* **1993**, *365*, 141. (b) Caneschi, A.; Gatteschi, D.; Sessoli, R.; Barra, A. L.; Brunel, L. C.; Guillot, M. *J. Am. Chem. Soc.* **1991**, *113*, 5873.

(6) Kostakis, G. E.; Ako, A. M.; Powell, A. K. *Chem. Soc. Rev.* **2010**, *39*, 2238.

(7) (a) Abbas, G.; Lan, Y.; Kostakis, G. E.; Wernsdorfer, W.; Anson, C. E.; Powell, A. K. *Inorg. Chem.* **2010**, *49*, 8067. (b) Sessoli, R.; Powell, A. K. *Coord. Chem. Rev.* **2009**, *253*, 2328. (c) Papatriantafyllopoulou, C.; Wernsdorfer, W.; Abboud, K. A.; Christou, G. *Inorg. Chem.* **2011**, *50*, 421. (d) Bencini, A.; Benelli, C.; Caneschi, A.; Dei, A.; Gatteschi, D. *Inorg. Chem.* **1986**, *25*, 572. (e) Caneschi, A.; Ferraro, F.; Gatteschi, D.; Rey, P.; Sessoli, R. *Inorg. Chem.* **1990**, *29*, 1756.(f) Sorace, L.; Benelli, C.; Gatteschi, D. *Chem. Soc. Rev.* DOI:10.1039/C0CS00185F

(8) (a) Tang, J. K.; Hewitt, I.; Madhu, N. T.; Chastanet, G.; Wernsdorfer, W.; Anson, C. E.; Benelli, C.; Sessoli, R.; Powell, A. K. *Angew. Chem., Int. Ed.* **2006**, *45*, 1729. (b) Chibotaru, L. F.; Ungur, L.; Soncini, A. *Angew. Chem., Int. Ed.* **2008**, *47*, 4126. (c) Hussain, B.; Savard, D.; Burchell, T. J.; Wernsdorfer, W.; Murugesu, M. *Chem. Commun.* **2009**, 1100. (d) Gamer, M. T.; Lan, Y. H.; Roesky, P. W.;

Powell, A. K.; Clérac, R. *Inorg. Chem.* **2008**, *47*, 6581. (e) Chen, Z.; Zhao, B.; Cheng, P.; Zhao, X. Q.; Shi, W.; Song, Y. *Inorg. Chem.* **2009**, *48*, 3493. (f) Bernot, K.; Luzon, J.; Bogani, L.; Etienne, M.; Sangregorio, C.; Shanmugam, M.; Caneschi, A.; Sessoli, R.; Gatteschi, D. *J. Am. Chem. Soc.* **2009**, *131*, 5573. (g) Bernot, K.; Pointillart, F.; Rosa, P.; Etienne, M.; Sessoli, R.; Gatteschi, D. *Chem. Commun.* **2010**, *46*, 6458. (h) Poneti, G.; Bernot, K.; Bogani, L.; Caneschi, A.; Sessoli, R.; Wernsdorfer, W.; Gatteschi, D. *Chem. Commun.* **2007**, 1807.

(9) (a) Bi, Y. F.; Wang, X. T.; Liao, W. P.; Wang, X. W.; Deng, R. P.; Zhang, H. J.; Gao, S. *Inorg. Chem.* **2009**, *48*, 11743. (b) Ishikawa, N.; Sugita, M.; Wernsdorfer, W. *J. Am. Chem. Soc.* **2005**, *127*, 3650. (c) Osa, S.; Kido, T.; Matsumoto, N.; Re, N.; Pochaba, A.; Mrozinski, J. *J. Am. Chem. Soc.* **2004**, *126*, 420.

(10) (a) Zheng, Y. Z.; Lan, Y.; Anson, C. E.; Powell, A. K. *Inorg. Chem.* **2008**, *47*, 10813. (b) Lin, P.-H.; Burchell, T. J.; Ungur, L.; Chibotaru, L. F.; Wernsdorfer, W.; Murugesu, M. *Angew. Chem., Int. Ed.* **2009**, *48*, 9489.

(11) (a) Ishikawa, N.; Sugita, M.; Ishikawa, T.; Koshihara, S.; Kaizu, Y. *J. Am. Chem. Soc.* **2003**, *125*, 8694. (b) AlDamen, M. A.; Clemente-Juan, J. M.; Coronado, E.; Martí-Gastaldo, C.; Gaita-Ariño, A. *J. Am. Chem. Soc.* **2008**, *130*, 8874. (c) Jiang, S. D.; Wang, B. W.; Su, G.; Wang, Z. M.; Gao, S. *Angew. Chem., Int. Ed.* **2010**, *49*, 7448. (d) Jiang, S. D.; Wang, B. W.; Sun, H. L.; Wang, Z. M.; Gao, S. *J. Am. Chem. Soc.* **2011**, *133*, 4730.

(12) Ke, H.; Gamez, P.; Zhao, L.; Xu, G. F.; Xue, S.; Tang, J. K. *Inorg. Chem.* **2010**, *49*, 7549.

(13) Galloway, K. W.; Whyte, A. M.; Wernsdorfer, W.; Sanchez-Benitez, J.; Kamenev, K. V.; Parkin, A.; Peacock, R. D.; Murrie, M. *Inorg. Chem.* **2008**, *47*, 7438.

(14) Isele, K.; Gigon, F.; Williams, A. F.; Bernardinelli, G.; Franz, P.; Decurtins, S. *Dalton Trans.* **2007**, 332.

(15) Yang, E. C.; Wernsdorfer, W.; Zakharov, L. N.; Karaki, Y.; Yamaguchi, A.; Isidro, R. M.; Lu, G. D.; Wilson, S. A.; Rheingold, A. L.; Ishimoto, H.; Hendrickson, D. N. *Inorg. Chem.* **2006**, *45*, 529.

(16) Moragues-Canovas, M.; Helliwell, M.; Ricard, L.; Riviere, E.; Wernsdorfer, W.; Brechin, E.; Mallah, T. *Eur. J. Inorg. Chem.* **2004**, 2219.

(17) Lin, P.-H.; Burchell, T. J.; Clérac, R.; Murugesu, M. *Angew. Chem., Int. Ed.* **2008**, *47*, 8848.

(18) Costes, J. P.; Laussac, J. P.; Nicodème, F. *J. Chem. Soc., Dalton Trans.* **2002**, 2731.

(19) (a) Liu, Q. C.; Ding, M. X.; Lin, Y. H.; Xing, Y. *Acta Crystallogr.* **1997**, *C53*, 1671. (b) Ambroziak, K.; Rozwadowski, Z.; Dziembowska, T.; Bieg, B. *J. Mol. Struct.* **2002**, *615*, 109.

(20) Stites, J. G.; McCarty, C. N.; Quill, L. L. *J. Am. Chem. Soc.* **1948**, *70*, 3142.

(21) Sheldrick, G. M. *SADABS. Program for Empirical Absorption correction of Area Detector Data*; University of Göttingen: Göttingen, Germany, 1996.

(22) (a) Sheldrick, G. M. *SHELXS-97, Program for X-ray Crystal Structure Solution*; University of Göttingen: Göttingen, Germany, 1997. (b) Sheldrick, G. M. *SHELXL-97, Program for X-ray Crystal Structure Refinement*; University of Göttingen: Göttingen, Germany, 1997.

(23) Adam, S.; Ellern, A.; Seppelt, K. *Chem.—Eur. J.* **1996**, *2*, 398.

(24) (a) Cole, K. S.; Cole, R. H. *J. Chem. Soc.* **1941**, *9*, 341. (b) Aubin, S. M. J.; Sun, Z.; Pardi, L.; Krzystek, J.; Folting, K.; Brunel, L. J.; Rheingold, A. L.; Christou, G.; Hendrickson, D. N. *Inorg. Chem.* **1999**, *38*, 5329.

(25) Long, J.; Habib, F.; Lin, P.-H.; Korobkov, I.; Enright, G.; Ungur, L.; Wernsdorfer, W.; Chibotaru, L. F.; Murugesu, M. *J. Am. Chem. Soc.* **2011**, *133*, 5328.

(26) (a) Wernsdorfer, W.; Bhaduri, S.; Boskovic, C.; Christou, G.; Hendrickson, D. N. *Phys. Rev. B* **2002**, *65*, 180403. (b) Wernsdorfer, W.; Chakov, N. E.; Christou, G. *Phys. Rev. Lett.* **2005**, *95*, 037203.